Available online at www.sciencedirect.com
ScienceDirect
Tectonophysics 431 (2007) 15–21
TECTONOPHYSICS
www.elsevier.com/locate/tecto

Surface oscillations — A possible source of fracture induced electromagnetic radiation

A. Rabinovitch [a,b], V. Frid [a,c,*], D. Bahat [a,c]

[a] The Deichmann Rock Mechanics Laboratory of the Negev, Ben Gurion University of the Negev, Beer Sheva, Israel
[b] Physics Department, Ben Gurion University of the Negev, Beer Sheva, Israel
[c] Geological and Environmental Sciences Department, Ben Gurion University of the Negev, Beer Sheva, Israel

Received 6 December 2005; received in revised form 25 April 2006; accepted 20 May 2006
Available online 27 November 2006

Abstract

Radio frequency electromagnetic radiation (EMR) registered hundreds of kilometres away from an earthquake epicentre is detected hours before earthquakes. Yet, accurate earthquakes prediction by their self-induced EMR still remains in its infancy due in part to the lack of understanding of EMR's origin. Here we present a viable model of this origin, according to which EMR is emitted by an oscillating dipole created by ions moving collectively as a surface wave on both sides of the crack; when the crack halts, the EMR pulse amplitude decays by interaction with bulk phonons. The model is shown to be able to provide crack dimensions and velocities, to explain some general similarities of different fracturing processes and indicate the existence of a general failure mechanism. Results raise the hope of developing an EMR based *genuine* earthquake prediction system.

Keywords: Electromagnetic radiation; Fracturing; Earthquake

1. Introduction

Earthquakes (EQ) constitute one of the most devastating natural hazards. Therefore a method for their prediction was sought for by geophysicists for a long time (Wyss, 1997). Of all possible prediction methods investigated thus far, none has been fully successful (Geller, 1997). Seismic precursors have extensively been studied, but so far, no effective warning system based on them has been obtained (Wyss, 1997, 2001). It is well established that EQ nucleate in focal zones (e.g. Rechez, 1999; Bahat et al., 2001), where cracks accelerate in less than a microsecond (Marder and Fineberg, 1996; Geller, 1997) and are followed by changes of the electromagnetic field in a wide range of frequencies from ~DC to light waves (Bahat et al., 2005 and refs therein). Our interest here is in the radio frequency range (EMR) (Gokhberg et al., 1982; Hayakawa et al., 1993; Rikitake, 1997; Fujinawa and Takahasi, 1998; Roeloffs, 1999; Kapiris et al., 2004).

The EMR signals, being emitted at the embryonic stages (nucleation) of an EQ, have a high potential of being used as EQ predictors but no progress in the use of this phenomenon as an EQ predictor was achieved due in part to the fact that the mechanism of EMR excitation was hitherto obscured.

We have conducted our experiments with dry specimens to avoid water ions interference and demonstrated

* Corresponding author. Geological and Environmental Sciences Department, Ben Gurion University of the Negev, Beer Sheva, Israel.
E-mail address: vfrid@bgu.ac.il (V. Frid).

0040-1951/$ - see front matter © 2006 Elsevier B.V. All rights reserved.
doi:10.1016/j.tecto.2006.05.027

(Frid et al., 2003) the inadequacy of all former "theories". Here we provide a viable model for the origin of the EMR, a model which could become the sought-for stepping-stone for a new era in the field.

2. Model of electromagnetic radiation

We maintain that polarization and acoustic emission (AE) are processes not related to the EMR discussed here. As for polarization, this process has been considered in Rabinovitch et al. (2003) and shown to lead to completely different pulse shapes. While acoustic emission, to say the least, always appears at a later time than that of the EMR.

A worthy model of the presently discussed EMR origin has to agree with the following four general characteristics based on the accumulated observations obtained in this field in the last four decades:

1. It should be invariant to a change of the material type (man-and non man-made) and to the loading mode (Rabinovitch et al., 2002a; Bahat et al., 2002; Frid et al., 2003).
2. It has to preserve symmetry, namely no preferred crack side should obtain a specific charge (charge neutrality); although some papers (e.g. Gershenzon et al., 1985) describe the phenomenon of "stress induced polarization", which could have been used as a precursor to EMR emanation during the cracking process, these reports are rare and no real explanation of the symmetry breaking is provided.
3. It has to provide a method by which measured crack parameters associated with the failure can be obtained.
4. It has to describe the shape of EMR signals in a way which is independent on the scale of the fractures inducing them.

An EMR mechanism adhering to these criteria is briefly presented here. In this model it is assumed that, following the breaking of bonds by the moving fracture, the atoms on both created sides are moved to "non-equilibrium" positions relative to their steady state ones and oscillate around them (Fig. 1). Lines of oscillating atoms move together and, being connected to atoms around them (both in the forward direction and on their side), the latter also participate in the movement. The ensuing vibrations are surface vibrational waves (SVW) where positive charges move together in a diametrically opposite phase to the negative ones while decaying exponentially into the material, like Rayleigh waves. The resulting oscillating electric dipoles act as the source of the EMR. The wave's amplitude decays by an interaction with bulk phonons.

As an example, we consider a crack propagating under a compressive load. The crack, usually of constant width, attains rapidly a final constant velocity, v_{cr}, propagates for a time period, T, while keeping this velocity, and then halts abruptly.

We neglect the transitional periods, assuming $v=v_{cr}$ for $0<t\le T$ and zero otherwise. Thus, within the interval $[0,T]$, during a time increment dt, the amplitude "A" of the envelope of the EMR decreases (by interaction with phonons) to $A(t)\left(1-\frac{dt}{\tau}\right)$, where τ is the decay time, and

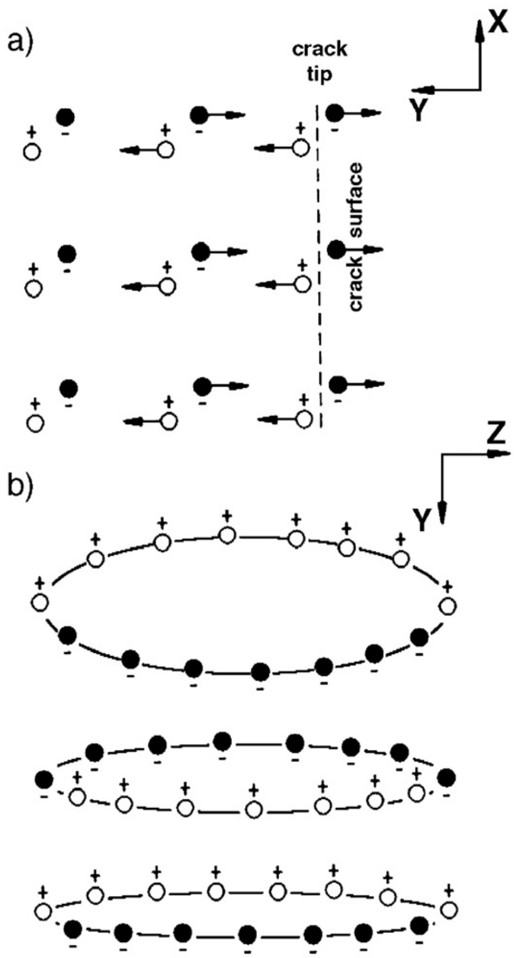

Fig. 1. a) A schematic SVW wave of a crack surface (a similar wave propagates on the other surface) at a specific time. Crack surface is in the '*xz*' plane and the crack moves in the '*x*' direction. Note that normal modes of charge separation can either be transverse (shown here) or longitudinal with respect to the surface, with appropriate EMR polarizations. Charge separation is oscillatory so that at a later time the dipole directions are reversed. b) Consequent decrease of the dipole amplitude created by the charge separation during crack propagation by interaction with bulk phonons.

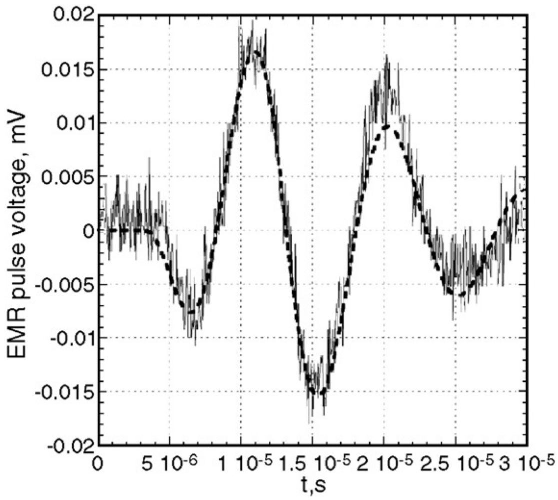

Fig. 2. An experimental EMR pulse (full line) and its numerical fit by Eq. (4) (dashed line).

is “replenished” by a term proportional to the number of severed bonds,, where ‘dx’ is the length increment of the crack in the interval ‘dt’ (dx=v_{cr}dt) and α is a coefficient relating the antenna output to ‘dx’. Obviously α depends on the cracking material (through the energy portion converted to EMR from the liberated bond breaking energy) and on the geometry of the experiment.

It follows that:

$$\frac{\partial A}{\partial t} = -\frac{A}{\tau} + \alpha v_{cr} \tag{1}$$

Hence,

$$A = \alpha v_{cr} \tau (1 - e^{-t/\tau}) \quad 0 \le t < T. \tag{2}$$

At t=T, the crack is assumed to halt, and the amplitude thereafter decays (again by interaction with phonons), resulting in

$$A = A(T) e^{-t/\tau} \quad t \ge T \tag{3}$$

Adding the oscillatory part, sin(ωt), yields the signals’ general shape (Rabinovitch et al., 1998):

$$A = \begin{cases} A_o \sin(\omega t)(1 - \exp(-t/\tau)), & t<T \\ A_o \sin(\omega t) \exp(-(t-T)/\tau)(1 - \exp(-T/\tau)), & t \ge T \end{cases} \tag{4}$$

where t is the time measured from the beginning of the pulse; T is the time to the maximum of the EMR pulse envelope, ω is the signal’s frequency, τ is the rise and fall times (decay times), which are assumed to be the same and $A_0 = \alpha v_{cr}$.

Several important results can immediately be deduced from the model:

a. Eq. (4) agrees well with experimentally measured shapes of EMR pulses ((Rabinovitch et al., 1998) and Fig. 2).

b. Eq. (4) implies that the maximum amplitude of EMR signals must be proportional to the crack velocity (Frid et al., 2006). Fig. 3 shows the results of crack velocity, v_{cr}, calculated by the Wallner lines method in glass, vs. maximum EMR amplitude. The regression line between them yields R^2=0.96.

c. Since the EMR pulse amplitude increases as long as the crack continues to grow and starts to decay when the crack halts, the time, T, from the start of the pulse up to its maximum should be proportional to the crack length ℓ (the crack velocity v_{cr} is almost constant) (Rabinovitch et al., 1998):

$$T \sim \frac{\ell}{v_{cr}} \tag{5}$$

This relation was indeed experimentally verified (Bahat et al., 2002) during transparent glass ceramic failure under compression.

d. Since surface waves decay in time as a result of an interaction with bulk phonons the decay time τ, which we identify with the rise and fall times of the EMR pulse, should be proportional to (Rabinovitch et al., 2003):

$$\tau \propto \frac{\rho^3 v^2}{\omega K^4} \tag{6}$$

where K is the local absolute temperature at the crack tip (much higher than room temperature), ρ is the material density, and v is the SVW wave velocity. The proportionality coefficient is considered to be a constant for the same material. Our investigations of different materials (Rabinovitch et al., 2003) showed that the

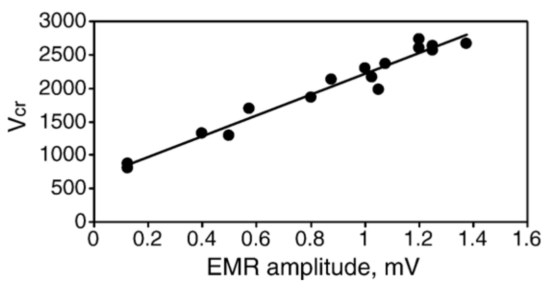

Fig. 3. Regression line between EMR pulse amplitude and incremental crack velocity measured by a Wallner lines analysis in an experiment on glass under tension.

slopes of τ vs. ω are −1±0.1 (R^2=0.85–0.96), agreeing with Eq. (6) (Fig. 4).

e. If the half wavelength, $\lambda/2$, of the atomic perturbation creating the EMR is limited by the crack width 'b' (which is assumed to be a constant) since at both sides of the crack atomic movements are restricted, then ((Rabinovitch et al., 2000; Frid et al., 2000) Fig. 1):

$$b \cong \lambda/2 = \frac{\pi v}{\omega} \quad (7)$$

The common slope of b vs. $1/\omega$ for glass, glass ceramics, granite and chalk was measured to be ≈0.93 (R^2=0.82) (Frid et al., 2003), which is very close to 1, in agreement with Eq. (7) (Fig. 5).

e. From Eqs. (5) and (7):

$$\frac{T}{\omega} \sim \frac{1}{\pi v_{cr} v} S \quad (8)$$

Where $S=\ell b$ is the crack area. Our measurements (Rabinovitch et al., 2000; Bahat et al., 2001) show a good agreement (R^2=0.9) between Eq. (8) and the experimental results (Fig. 6).

Our recent experiments have shown (Rabinovitch et al., 2005) that *friction* induces EMR signals in the frequency range of 20–25 MHz. The shape of these signals is similar to the ones of the same frequency range emanated during rock *fractures* (Rabinovitch et al., 1996) induced by material compression (Fig. 2). "Crack" sizes in friction, according to Eq. (7) come out to be on the order of 20 μm, implying that EMR from friction can be due to microfracturing of asperities on the rock surfaces, thus supporting the Bowden–Tabor model of friction (Bowden and Tabor, 2001).

Our investigations indicate that a *single cumulative global failure mechanism* may constitute the driving force for different fracturing processes (compression, tension, shear, impacts, percussion drilling and even medium scale collapse).

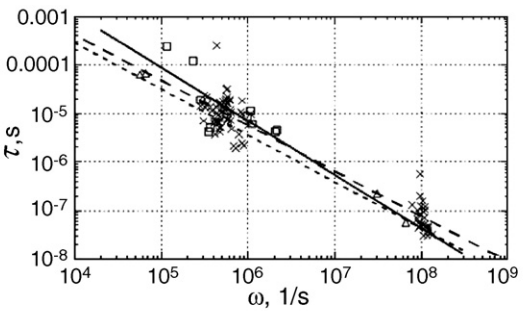

Fig. 4. The rise and fall time, τ, as a function of frequency, ω. The points are the experimental results of individual pulses, and the lines are the regression fitted lines. Results are for glass (Δ, ----); glass ceramics (□, —) and granite (x and – – –).

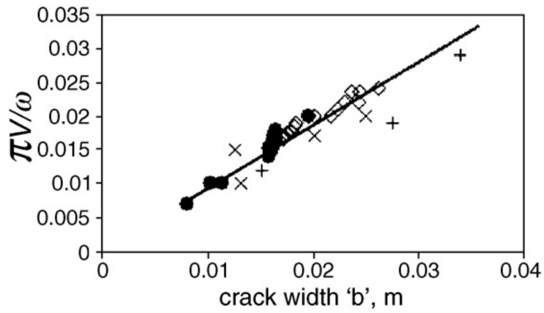

Fig. 5. The relation between reciprocal EMR frequency and fracture width for chalk (●), granite (◇), glass (+) and glass ceramics (x).

Our present EMR measurements in a direct tension experiment in glass failure has however created an interesting problem of consistency of the global mechanism. We first describe the results then pose the problem and discuss a possible solution. In these experiments the EMR pulses appear in two main different forms: "short" (total duration 0.5–6 μs, Fig. 7a) and "extended" (of larger duration — up to 20 μs, Fig. 7b). The shapes of the short individual pulses (Fig. 7a) are very similar to those observed in microfracturing during compression (Figs. 2) and during percussion drilling (Rabinovitch et al., 1996, 2000; Goldbaum et al., 2001; Rabinovitch et al., 2002a, 2004). However, the shapes of the extended signals (Fig. 7b) are completely different from those measured during the compression experiments (local tension/shear) (Fig. 2). They are very similar to those measured during flake creation induced by percussion drilling (Goldbaum et al., 2001): The extended signals in both cases are composed of strings of many individual short pulses, each of which is very similar in shape to pulse shapes observed during compression experiments, albeit of a higher frequency.

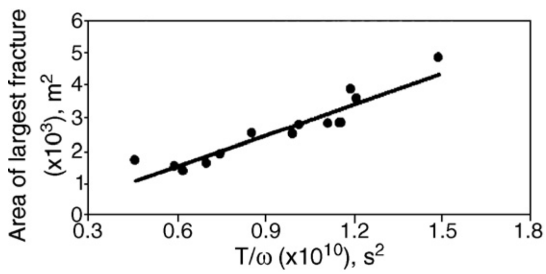

Fig. 6. Experimental maximal fracture areas vs. largest T'/ω values and a linear fit (R^2=0.9).

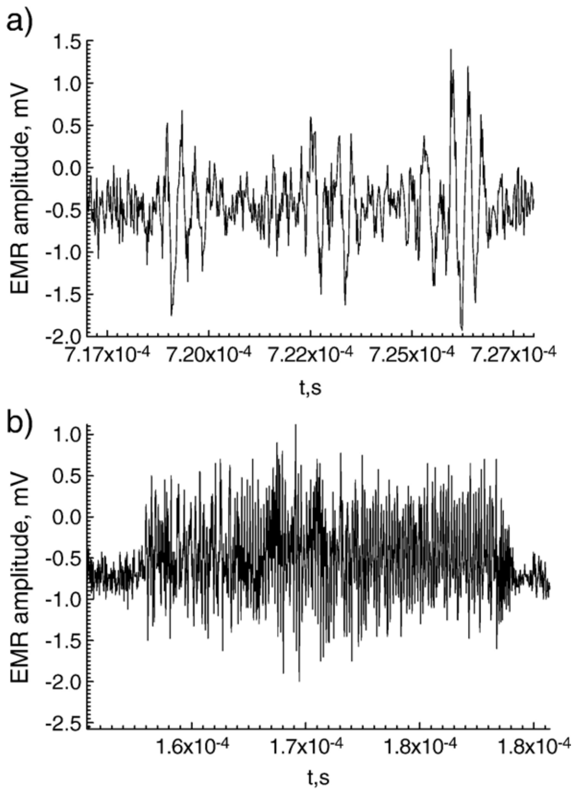

Fig. 7. a) Short EMR pulses excited by nucleating cracks during direct tension, note the high noise level; b) An extended EMR signal excited by the sample collapse under direct tension.

The basic question which arises is: why do EMR pulses during direct tension and drilling experiments emanate as strings and not as a single lengthy signal (Fig. 2) (which is the shape expected from a single lengthy fracture and is indeed the usual shape measured during lengthy fracturing under compressive loading)?

A possible explanation is that the fracturing process under direct (remote) tension has initiated at many different locations and coalesced to form a unified surface but emitted a distinct EMR pulse from each individual small fracture which combined into an extended signal.

This conclusion is confirmed by medium scale experiments in an underground mine (Frid and Vozoff, 2005) where EMR was used for monitoring an incipient roof fall. The failure process is usually preceded by numerous micro-cracks. An analysis of EMR records observed in these experiments showed that they consisted of extended EMR strings, each of which composed of numerous individual signals similar in shape to those measured by us in the lab and in open quarry during blasting (Rabinovitch et al., 2002a). It means that, when numerous cracking events take place with a short interval between them, extended chains of individual EMR signals are created which are quite similar to those emanated during the glass tension experiment. It seems therefore that our multi-scale hypothesis of the existence of a global failure mechanism can be true.

To check the existence of such a mechanism we analyzed two relationships that are known to be applicable for the characterization of multi-scale fracturing: the Gutenberg–Richter type law and the Benioff strain release relation. The Gutenberg–Richter law, that is valid for earthquakes, laboratory studies of acoustic emission (Lockner et al., 1991) and even for energy distributions of neutron starquakes (Kossobokov et al., 2000), was shown to be valid also for EMR amplitudes induced by rock (laboratory scale) failure (Rabinovitch et al., 2002b). In addition to this purely statistical law, the time dependent ‘‘cumulative Benioff strain-release’’ relation of all EMR signals registered during rock compression before collapse (Fig. 8) was shown (Rabinovitch et al., 2002b) to be very similar to the usual (EQ) ‘‘Benioff strain-release’’ graph. The slope in its middle part ($\alpha = 1.42$, $R^2 = 0.99$) is close to 1.43, the value found for EQ (Bowman et al., 1998) and logarithmic-periodic variations appear in the middle parts of the Benioff curves both for the EQ and EMR measurements. Similar results were obtained during medium scale EMR investigations in underground mine (Frid and Vozoff, 2005).

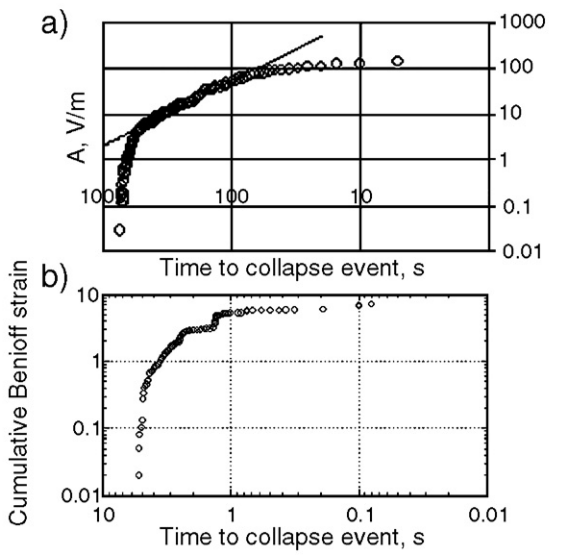

Fig. 8. The “Cumulative Benioff strain release” of a) amplitude of EMR signals registered during rock compression and b) seismic events prior to Superstition Hills (24.11.1987) EQ [22] vs. time before collapse (time is measured backwards from the moment of collapse).

3. Discussion

As was shown, all results of the hitherto performed experiments have substantiated the validity of the SVW model. Moreover, at the beginning of Section 2 we put forth four main characteristics that a credible model of EMR has to adhere to. We now consider each one of them in detail and check whether they apply to the present model.

1. The independency of the SVW model on material type and loading mode:

a. In contrast to the models of Misra (1977) and Gershenzon et al. (1985), no dislocations are included in the model and therefore it can be applied to both brittle and amorphous materials. b. The basic shape of the EMR signals predicted by our model (Eq. (4)), is indeed the one observed in failure experiments excited by different methods, such as compression, drilling and blasting and does not change with the (dynamic/quasi-static) loading mode (Rabinovitch et al., 2002a).

2. Neutrality of crack surfaces: charge neutrality is assured here by the mechanism of SVW, in which only the dipoles oscillate back and forth. Therefore no 'mosaic' cancellation of the EMR amplitude is expected (in contrast to the model of Khatiashvili (1984). Note that although the AE and crack speed are much smaller than the EMR one, the crack front or the AE wave front (which were invoked as causing EMR in these models) pass simultaneously through several differently polarized zones which would lead to either large fluctuations or complete annihilation of the EMR amplitude.

3. Extracting fracture parameters: our model enables us to calculate fracture length, width, area, time of decay of EMR signals and even the velocity of crack propagation. For example, experimental EMR frequencies do agree with those predicted by the SVW, namely they are inversely proportional to the width of the crack. The spectrum is definitely not of a 'white noise' type as predicted by the "break-down" model (Miroshnishencko and Kuksenko, 1980).

4. Independence on failure scale: this principle was confirmed by our micro-scale (lab experiments) and medium scale (in an open quarry and in underground mine) investigations. Confirmation of this principle in the field scale is the aim of further investigations. These will hopefully constitute the essential step for the use of EMR for earthquake prediction.

5. The polarization of the EMR itself, as predicted by the normal modes (Fig. 1) was actually confirmed by the field measurements carried out by Lichtenberger (2006).

The main problems encountered in the use of EMR as a tool for predicting EQ's arise from the difficulties to measure the specific EMR from EQ nucleation in the background of spherics, thunderstorms, ionospheric disturbance and anthropogenic noises. Our model may help in distinguishing the "correct" EMR from "spurious" ones by the shape and properties of the former, and thus lead to the ability of using it in an EQ predictive capacity. One important, hitherto unresolved problem in the use of this method is that of the EMR propagation through the lithosphere and the ability to detect it by conventional means.

Acknowledgements

This research was supported by the Israel Science Foundation (No. 93/02) and the Earth Sciences Administration of the Ministry of Energy and Infrastructure (No. 22-17-008). We wish to thank Prof. K. Vosoff and Dr. M. Lichtenberger for their very helpful remarks that significantly improved this paper.

References

Bahat, D., Rabinovitch, A., Frid, V., 2001. Fracture characterization of chalk in uniaxial and triaxial tests by rock mechanics, fractographic and electromagnetic radiation methods. J. Struct. Geol. 23, 1531–1547.

Bahat, D., Frid, V., Rabinovitch, A., Palchik, V., 2002. Exploration via electromagnetic radiation and fractographic methods of fracture properties induced by compression in glass-ceramic. Int. J. Fract. 116, 179–194.

Bahat, D., Rabinovitch, A., Frid, V., 2005. Tensile fracturing in rocks. Tectonofractographic and Electromagnetic Radiation Methods. Springer, Heidelberg. 569 pp.

Bowden, F.P., Tabor, D., 2001. The Friction and Lubrication of Solids. Oxford Univ. Press, New York.

Bowman, D.D., Ouillon, G., Sammis, C.G., Sornette, D., Sornette, A., 1998. An observational test of the critical earthquake concept. J. Geophys. Res. 103 (24), 24359–24372.

Frid, V., Vozoff, K., 2005. Electromagnetic radiation induced by mining rock failure. Int. J. Coal Geol. 64, 57–65.

Frid, V., Bahat, D., Goldbaum, J., Rabinovitch, A., 2000. Experimental and theoretical investigation of electromagnetic radiation induced by rock fracture. Isr. J. Earth-Sci. 49, 9–19.

Frid, V., Rabinovitch, A., Bahat, D., 2003. Fracture induced electromagnetic radiation. J. Phys., D, Appl. Phys. 36, 1620–1628.

Frid, V., Rabinovitch, A., Bahat, D., 2006. Crack velocity measurement by induced electromagnetic radiation. Phys. Lett., A 356, 160–163.

Fujinawa, Y., Takahashi, K., 1998. Electromagnetic radiations associated with major earthquakes. Phys. Earth Planet. Inter. 105 (3–4), 249–259.

Geller, R.J., 1997. Earthquake prediction: a critical review. Geophys. J. Int. 131, 425–450.

Gershenzon, N., Zilpimiani, D., Maguladze, P., 1985. Electromagnetic radiation from crack tip during ionic crystals fracture. Dokl. Akad. Nauk SSSR 248, 1077–1081.

Gokhberg, M., Yoshino, T., Morgunov, V., 1982. Results of recording operative electromagnetic earthquake precursor in Japan. Phys. Solid Earth 18, 144–146.

Goldbaum, J., Frid, V., Rabinovitch, A., Bahat, D., 2001. Electromagnetic radiation induced by percussion drilling. Int. J. Fract. 111, L15–L20.

Hayakawa, M., Tomizawa, I., Ohta, K., 1993. Direction finding of precursory radio emissions associated with earthquakes: a proposal. Phys. Earth Planet. Inter. 77, 127–135.

Kapiris, P., Chelidze, T., Eftaxias, K., 2004. Electromagnetic Signature of prefracture Criticality in Heterogeneous Media. Phys. Rev. Lett. 92, 0657021–0657024.

Khatiashvili, N., 1984. The electromagnetic effect accompanying the fracturing of alkaline halide crystals and rocks. Phys. Solid Earth 20, 656–661.

Kossobokov, V.G., Keilis-Borok, V.I., Cheng, B., 2000. Similarities of multiple fracturing on a neutron star and on the Earth. Phys. Rev. E Stat. Phys. Plasmas Fluids Relat. Interdiscip. Topics 61, 3529–3533.

Lichtenberger, M., 2006. Neues Jahrb. Geol. Palaontol. Abh. 238 (2), 279–312.

Lockner, D.A., Byerlee, J.D., Kuksenko, V., Ponomarev, A., Sidorin, A., 1991. Quasi-static fault growth and shear fracture energy in granite. Nature 350, 39–42.

Marder, M., Fineberg, J., 1996. How things break. Phys. Today 49, 24–29.

Miroshnishencko, M., Kuksenko, V., 1980. Emission of electromagnetic pulses during nucleation of cracks in solid insulators. Sov. Phys., Solid State 22 (5), 895–896.

Misra, A., 1977. Physical model for the stress-induced electromagnetic effect in metals. Appl. Phys. 16, 195–199.

Rabinovitch, A., Bahat, D., Frid, V., 1996. Emission of electromagnetic radiation by rock fracturing. Z. Geol. Wiss. 24, 361–368.

Rabinovitch, A., Frid, V., Bahat, D., 1998. Parametrization of electromagnetic radiation pulses obtained by triaxial fracture in granite samples. Philos. Mag. Lett. 77, 289–293.

Rabinovitch, A., Frid, V., Bahat, D., Goldbaum, J., 2000. Fracture area calculation from electromagnetic radiation and its use in chalk failure analysis. Int. J. Rock Mech. Min. Sci. 37, 1149–1154.

Rabinovitch, A., Bahat, D., Frid, V., 2002a. Similarity and dissimilarity of electromagnetic radiation from carbonate rocks under compression, drilling and blasting. Int. J. Rock Mech. Min. Sci. 39, 125–129.

Rabinovitch, A., Frid, V., Bahat, D., 2002b. Gutenberg–Richter type relation for laboratory fracture induced electromagnetic radiation. Phys. Rev., E Stat. Phys. Plasmas Fluids Relat. Interdiscip. Topics 65, 011401–011404.

Rabinovitch, A., Frid, V., Goldbaum, J., Bahat, D., 2003. Polarization–depolarization process in glass during percussion drilling. Philos. Mag. 83, 2929–2940.

Rabinovitch, A., Shay, A., Liraz, R., Frid, V., Bahat, D., 2005. Electromagnetic radiation emitted during friction process. Int. J. Fract. 131, L21–L27.

Rechez, Z., 1999. Mechanisms of slip nucleation during earthquakes. Earth Planet. Sci. Lett. 170, 475–486.

Rikitake, T.J., 1997. Nature of electromagnetic radiation precursory to an earthquake. Geomag. Geoelectr. 49, 1153–1163.

Roeloffs, E., 1999. Radon and rock deformation. Nature 399, 104.

Wyss, M., 1997. Cannot earthquakes be predicted? Nature 278, 487.

Wyss, M., 2001. Why is earthquake prediction research not progressive faster? Tectonophysics 338, 217–223.